Available online at www.sciencedirect.com

ScienceDirect

IFAC-PapersOnLine 49-19 (2016) 486–493

Obstacle Avoidance by Steering and Braking with Minimum Total Vehicle Force

Amrik Singh Phuman Singh * Osamu Nishihara **

* Department of Systems Science, Kyoto University, Kyoto, Japan (e-mail: amrik.singh.46u@st.kyoto-u.ac.jp).
** Department of Systems Science, Kyoto University, Kyoto, Japan (e-mail: nishihara@i.kyoto-u.ac.jp).

Abstract: In this study of automatic obstacle avoidance maneuver, a fast and precise algorithm for solving a two-point boundary value problem (TPBVP) is developed. This algorithm realizes optimal control by minimizing the total vehicle force using integrated steering and braking control. Such optimal control is characterized by three nonlinear equations that result from the application of the necessary conditions for optimality. These highly nonlinear simultaneous equations are nondimensionalized, and algebraic manipulations are performed for simplification. As a result, they are reduced to a single nondimensionalized equation with the dimensionless final time as an unknown and aspect ratio as an input that describes the relative position between the obstacle and vehicle. For a fast and robust solution process, a search interval for a numerical root solving method is set using approximating polynomials. Based on the solution of the dimensionless final time, the dimensionless total vehicle force and dimensionless jerk, both of which are essential aspects of collision avoidance maneuver, can be easily computed.

Keywords: automotive control, jerk, nondimensionalization, optimal control, vehicle dynamics.

1. INTRODUCTION

In automotive engineering, driver assistance systems for safety are considered the most essential field of study. Collision avoidance systems based on automatic braking are already available in production vehicles. Collision avoidance by pure braking is effective for cases of low vehicle speed with high tire-road friction coefficients. Obstacle avoidance by steering offers better performance for higher vehicle speed and/or on wet road surfaces. With full utilization of the vehicle friction circle, the integration of steering and braking has been demonstrated to be more effective than pure steering (Hattori et al., 2008).

Various objective functions for the optimal control of the integrated steering and braking have been studied. Shiller and Sundar (1998) used minimum longitudinal avoidance distance. In a study by Fujioka et al. (2008), a minimization of collision risk was suggested. This collision risk consists of a risk function that depends on the obstacle location, a function of time-to-collision or longitudinal avoidance distance, and a penalty function of longitudinal and lateral accelerations. The penalty function provides smooth acceleration/braking and steering actions. Minimization of the time integral of the sum of squared tire workloads, and front-wheel steering angle rate was studied by Horiuchi et al. (2006).

In a recent study, a minimization of the total vehicle force problem was proposed by Ohmuro and Hattori (2010). By minimizing the total vehicle force, the force margin is maximized, and this allows operations with some safety margin. Because of the availability of friction estimation methods, we can assume online monitoring of the maximum vehicle force. In order to estimate the friction coefficient, Muller et al. (2003) used friction coefficient versus slip data for the low slip region; Alvarez et al. (2004) used a first-order dynamic friction model called the LuGre model; Wang et al. (2004) used linear and non-linear models for low and high slips, respectively; and Nishihara and Kurishige (2011) used the grip margin derived from the brush model. Note that the obstacle avoidance maneuver can be realized if the required total force does not exceed the maximum vehicle force.

In the previous study (Ohmuro and Hattori, 2010), the application of the optimal control theory results in a two-point boundary value problem (TPBVP), that is reduced to a system of highly nonlinear equations. Because of the difficulties expected in the online solution of these highly nonlinear equations, they proposed a pair of two-dimensional maps that provide the total vehicle force along with the direction angle that constitutes the optimal control inputs. In general, use of these maps leads to inaccurate solutions, particularly in the case where the output is very sensitive to the inputs. Such accuracy could be improved by increasing map resolution at the expense of large data storage space.

For one equation in one unknown, fast root finding methods, such as Newton's, secant, and inverse quadratic interpolation, are available. Brent's method is a hybrid algorithm that includes the very stable bisection method, and is known for its combined efficiency and robustness (Brent, 1971). To a system of nonlinear equations, application of Newton's or Broyden's method may offer speed; however, there is no guarantee of convergence. Reduction to one equation in one unknown is preferable because stable con-

10.1016/j.ifacol.2016.10.638

vergence is mostly guaranteed with a sufficiently narrow interval determined with an approximate solution to the equation.

In this paper, minimization of the total vehicle force for the obstacle avoidance problem is reduced to finding the solution of one equation in one unknown. In order to estimate the initial guess for the root solving method, Chebyshev and least squares function approximations are performed. The dimensionless final time is obtained with high precision using Brent's method, and this leads to the determination of optimal control that is as precise as required.

2. PROBLEM FORMULATION

2.1 Obstacle Avoidance Problem

Figure 1 shows a vehicle that moves on a straight road with initial vehicle longitudinal velocity v_{x0}, and initial lateral velocity v_{y0}, at a given position. The vehicle performs a lane change in order to avoid an obstacle blocking its forward path. The longitudinal distance to the obstacle is denoted by x_f. The lateral distance at final time t_f, is given as y_f. For simplicity, the vehicle is treated as a particle with mass m. In this problem, total vehicle force F_t, is to be minimized for the lane change maneuver.

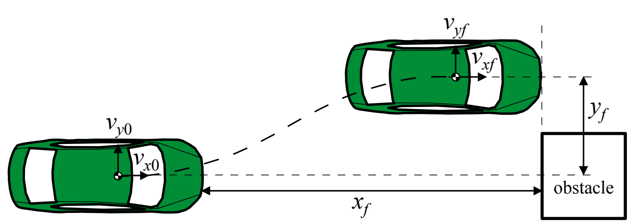

Fig. 1. Schematic diagram of lane change maneuver

Figure 2 the trade-off between total longitudinal force X_t, and total lateral force Y_t. These are the forces that a vehicle generates at a given instant. Total vehicle force F_t, is assumed to be time invariant and limited by the maximum vehicle force $F_{\max}$, that is expressed as the product of tire-road friction coefficient μ, and vehicle normal load $Z_t = mg$. Maximum force $F_{\max} = \mu Z_t$ represents the tire grip limit. Once the longitudinal and lateral vehicle forces are evaluated, tire-forces distribution schemes (Nishihara and Higashino, 2013; Ono et al., 2006) can be utilized to calculate the front and rear wheel steering angles and braking torques, but this phase is not within the scope of this study.

2.2 Optimal Control Problem Formulation

An optimal control theory is utilized for the obstacle avoidance problem (Bryson and Ho, 1975). A system model is given as

$$\dot{\boldsymbol{x}}(t) = \boldsymbol{f}(\boldsymbol{x}(t), \boldsymbol{u}(t), t) \quad \boldsymbol{x}(t_0) = \boldsymbol{x_0} \tag{1}$$

where $\boldsymbol{x}(t)$ and $\boldsymbol{u}(t)$ denote, respectively, the n and m dimensional vectors of the state and control variables. The control inputs and corresponding states are

$$\boldsymbol{u}(t) = \left[\frac{F_t}{m} \;\; \varphi\right]^T \tag{2}$$

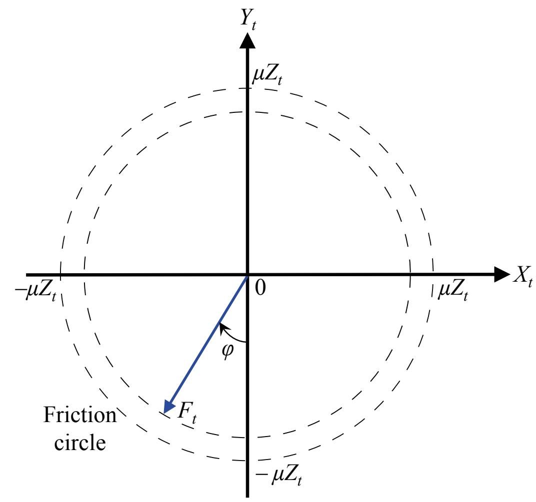

Fig. 2. Total vehicle force bounded by friction circle

$$\boldsymbol{x}(t) = [x(t) \;\; \dot{x}(t) \;\; y(t) \;\; \dot{y}(t)]^T \tag{3}$$

The initial conditions of the states are

$$\boldsymbol{x}(t_0) = [0 \;\; v_{x0} \;\; 0 \;\; v_{y0}]^T \tag{4}$$

The objective function for the obstacle avoidance lane change problem is

$$\min_{\boldsymbol{u}(t)} J = F_t \tag{5}$$

The terminal constraint is written as

$$\boldsymbol{\psi}(\boldsymbol{x}(t), t) = [x(t) - x_f \;\; y(t) - y_f \;\; \dot{y}(t)]^T \tag{6}$$

The longitudinal and lateral dynamics of the vehicle can be expressed as (7) and (8), respectively.

$$X_t\,(t) = m a_x\,(t) \tag{7}$$

$$Y_t\,(t) = m a_y\,(t) \tag{8}$$

where the longitudinal acceleration a_x, and lateral acceleration a_y, are written as

$$a_x\,(t) = -\frac{F_t}{m} \sin\varphi\,(t) \tag{9}$$

$$a_y\,(t) = -\frac{F_t}{m} \cos\varphi\,(t) \tag{10}$$

where

$$\tan\varphi(t) = \frac{-t + t_f}{-\nu_y t + \nu_y t_f + \nu_v} \tag{11}$$

Hattori and Ohmuro (2010) discussed three obstacle avoidance problems that are minimization of x_f, minimization of F_t, and maximization of y_f. These problems are related to each other such that their optimal solutions can be obtained by solving the same simultaneous equations with different parameter sets of given and unknown. We have derived a precise solution method for the minimization of x_f where $y(t_f) = y_f$ and $v_y(t_f) = 0$ are the terminal constraints, and F_t is assumed to be known prior to the lane change maneuver (Singh and Nishihara, 2016). In the present study, F_t is to be minimized for a given x_f. Note that the minimization of F_t is a dual problem of the minimization of x_f. Therefore, the simultaneous equations of the primal problem is used here. In Eqs. (12) to (16), the variables to be determined are Lagrange multiplier constants ν_y and ν_v, as well as final time t_f.

$$\frac{mv_{x0}}{F_t} - \frac{2\nu_y\nu_v M}{(1+\nu_y^2)^{3/2}} - \frac{\nu_y^2\nu_v}{1+\nu_y^2} - \frac{\sqrt{(\nu_y t_f+\nu_v)^2+t_f^2}}{1+\nu_y^2} = 0 \tag{12}$$

$$\frac{mv_{x0}t_f}{F_t} - \frac{mx_f}{F_t} + \frac{\nu_v^2(2\nu_y^2-1)M}{(1+\nu_y^2)^{5/2}} - \frac{3\nu_y\nu_v^2}{2(1+\nu_y^2)^2} - \frac{\left((1+\nu_y^2)t_f - 3\nu_y\nu_v\right)\sqrt{(\nu_y t+\nu_v)^2+t_f^2}}{2(1+\nu_y^2)^2} = 0 \tag{13}$$

$$\frac{mv_{y0}}{F_t} + \frac{2\nu_v M}{(1+\nu_y^2)^{3/2}} + \frac{\nu_y\nu_v}{1+\nu_y^2} - \frac{\nu_y\sqrt{(\nu_y t_f+\nu_v)^2+t_f^2}}{1+\nu_y^2} = 0 \tag{14}$$

$$\frac{mv_{y0}t_f}{F_t} - \frac{my_f}{F_t} - \frac{3\nu_y\nu_v^2 M}{(1+\nu_y^2)^{5/2}} - \frac{\nu_v^2(\nu_y^2-2)}{2(1+\nu_y^2)^2} - \frac{\sqrt{(\nu_y t_f+\nu_v)^2+t_f^2}\left(\nu_y t_f(1+\nu_y^2) - \nu_v(\nu_y^2-2)\right)}{2(1+\nu_y^2)^2} = 0 \tag{15}$$

where

$$M = \frac{1}{2}\ln\left(\frac{M_n}{M_d}\right) \tag{16}$$

with

$$M_n = \left(\nu_y + \sqrt{1+\nu_y^2}\right)^2 \left(\nu_v + t_f\sqrt{1+\nu_y^2} - \sqrt{(\nu_y t_f+\nu_v)^2+t_f^2}\right)$$

$$M_d = -\nu_v + t_f\sqrt{1+\nu_y^2} + \sqrt{(\nu_y t_f+\nu_v)^2+t_f^2}$$

By solving Eq. (12) with respect to F_t/m and substituting this solution into Eqs. (13) to (15), the remaining input variables are x_f, y_f, v_{x0}, and v_{y0}, and the unknowns referred to as the control parameters are ν_y, ν_v, and t_f. By applying Buckingham π theorem, the equations with seven original variables and two physical dimensions: length L and time T, can be expressed by five dimensionless variables. These dimensionless variables are expressed as the combination of original variables, as indicated in Table 1. Throughout this paper, π_x and τ_f are referred to as the ratio of the final lateral distance to the final longitudinal distance that can be referred to as the inverse aspect ratio and dimensionless final time, respectively.

Table 1. Dimensionless variables

Original variables	Dimensional space	Dimensionless variables
(v_{x0}, x_f, y_f)	$[\mathrm{LT}^{-1}]^0[\mathrm{L}]^{-1}[\mathrm{L}]^1$	$\pi_x = \frac{y_f}{x_f}$
(v_{x0}, x_f, v_{y0})	$[\mathrm{LT}^{-1}]^{-1}[\mathrm{L}]^0[\mathrm{LT}^{-1}]^1$	$\pi_v = \frac{v_{y0}}{v_{x0}}$
(v_{x0}, x_f, ν_y)	$[\mathrm{LT}^{-1}]^0[\mathrm{L}]^0$	$N_1 = \nu_y$
(v_{x0}, x_f, ν_v)	$[\mathrm{LT}^{-1}]^1[\mathrm{L}]^{-1}[\mathrm{T}]^1$	$N_2 = \frac{v_{x0}\nu_v}{x_f}$
(v_{x0}, x_f, t_f)	$[\mathrm{LT}^{-1}]^1[\mathrm{L}]^{-1}[\mathrm{T}]^1$	$\tau_f = \frac{v_{x0}t_f}{x_f}$

The equations that describe TPBVP are then rewritten in terms of these dimensionless variables. Algebraic manipulations are performed to reduce the original problem to a root finding problem of one variable equation, as given in Eq. (17). For simplicity, the vehicle is assumed to travel in the longitudinal direction at the point where the lane change maneuver is initiated, and therefore, v_{y0} is zero. Because of lack of space, the detailed derivation is not provided here.

$$\begin{aligned} &-2N_1N_2P\left(3N_2+2\pi_x R\right) - \sqrt{R}(N_2^2\left(N_1^2-2\right) \\ &+2N_1^2N_2\pi_x R - N_2Q\left(N_1^2-2\right) + QR\left(2\pi_x+N_1\tau_f\right)) = 0 \end{aligned} \tag{17}$$

where

$$R = 1+N_1^2 \tag{18}$$

$$Q = \sqrt{N_2^2+2N_1N_2\tau_f+R\tau_f^2} \tag{19}$$

$$P = \frac{1}{2}\ln\left(\frac{\left(N_1+\sqrt{R}\right)^2\left(N_2-Q+\tau_f\sqrt{R}\right)}{-N_2+Q+\tau_f\sqrt{R}}\right) \tag{20}$$

The cubic function of N_2 is given by the following equation:

$$a_3N_2^3+a_2N_2^2+a_1N_2+a_0 = 0 \tag{21}$$

where the coefficients are given as

$$a_3 = -256\pi_x^5\left(2+2\pi_x^2+\tau_f\left(2\tau_f-5\right)\right) \tag{22a}$$

$$\begin{aligned} a_2 = &-64\pi_x^4(4\pi_x^4+\left(\tau_f-2\right)^2\left(1+6\tau_f\left(\tau_f-1\right)\right) \\ &+4\pi_x^2\left(2+\tau_f\left(4\tau_f-7\right)\right)) \end{aligned} \tag{22b}$$

$$\begin{aligned} a_1 = &-64\pi_x^3\tau_f\left(2+2\pi_x^2+\tau_f\left(\tau_f-3\right)\right) \\ &\left(\left(\tau_f-2\right)^2\left(2\tau_f-1\right)+\pi_x^2\left(6\tau_f-4\right)\right) \end{aligned} \tag{22c}$$

$$\begin{aligned} a_0 = &-16\pi_x^2\tau_f^2\left(4\pi_x^2+\left(\tau_f-2\right)^2\right) \\ &\left(2+2\pi_x^2+\tau_f\left(\tau_f-3\right)\right) \end{aligned} \tag{22d}$$

The real root of this cubic equation is found to be

$$N_2 = -\frac{a_2}{3a_3} - \frac{2^{1/3}d_0}{3a_3\left(d_1+\sqrt{4d_0^3+d_1^2}\right)^{1/3}} + \frac{\left(d_1+\sqrt{4d_0^3+d_1^2}\right)^{1/3}}{3\left(2^{1/3}\right)a_3} \tag{23}$$

where

$$d_1 = -2a_2^3+9a_3a_2a_1-27a_3^2a_0 \tag{24a}$$

$$d_0 = -a_2^2+3a_3a_1 \tag{24b}$$

After algebraic manipulations, N_1 can be expressed as a linear function of τ_f.

$$N_1 = \frac{\tau_f-2}{2\pi_x} \tag{25}$$

After substituting Eqs. (23) and (25) into Eq. (17), τ_f remains as a single unknown. To determine τ_f, an iterative method should be applied because of the nonlinear nature of this equation. The best approach would be an application of hybrid method, such as Brent's method (Brent, 1971), that combines the fast open methods and reliable bisection method for root finding. In the root solving method, it is most likely that a smaller initial interval would yield faster convergence to the solution. The next section describes the function approximation methods for estimating initial search interval.

3. POLYNOMIAL APPROXIMATIONS OF DIMENSIONLESS FINAL TIME

3.1 Chebyshev Approximation

A previous study (Ohmuro and Hattori, 2010) used a lookup table for the solution of similar simultaneous equations. Lookup tables are commonly used with some interpolation technique, but the combination does not always provide good results. In this study, we use the Chebyshev approximation method known for its easy realization of the substantial minimization of the maximum error (Press et al., 1992). The trigonometric form of the Chebyshev polynomial is

$$T_n(x) = \cos(n \arccos x) \tag{26}$$

The recurrence relation for Chebyshev polynomials is

$$\begin{aligned} T_{n+1}(x) &= 2xT_n(x) - T_{n-1}(x), \quad n = 1, 2, ...; \\ T_0(x) &\equiv 1, \quad T_1(x) \equiv x. \end{aligned} \tag{27}$$

Chebyshev polynomials obey the discrete orthogonality in interval $[-1, 1]$.

$$\sum_{k=1}^{m} T_i(x_k)\, T_j(x_k) = \begin{cases} 0, & i \neq j \\ m/2, & i = j \neq 0 \\ m, & i = j = 0 \end{cases} \tag{28}$$

Given a function $f(x)$ defined in interval $[-1, 1]$, and N coefficients $c_j, j = 0, ..., N-1$, are

$$c_j = \frac{2}{N} \sum_{k=1}^{N} f(x_k)\, T_j(x_k) \tag{29}$$

where

$$T_j(x_k) = \cos\left(\frac{\pi j (2k-1)}{2N}\right) \tag{30}$$

the Chebyshev approximating polynomial of degree $N-1$ for $f(x)$ over interval $[-1, 1]$ is expressed as

$$f(x) \approx -\frac{1}{2}c_0 + \sum_{k=0}^{N-1} c_k T_k(x) \tag{31}$$

This approximation with a truncation realizes a smooth spreading out of the error, and becomes very close to the minimax polynomial with the smallest maximum deviation from $f(x)$. Nearness to the minimax polynomial and easiness of computation make the Chebyshev approximating polynomial a preference for practical work.

The approximation problem on an arbitrary interval $[x_0, x_1]$ can be performed with some linear variable transformation; the problem is reformulated on interval $[-1, 1]$.

$$\tilde{x} = \frac{x - \frac{1}{2}(x_1 + x_0)}{\frac{1}{2}(x_1 - x_0)} \tag{32}$$

The quadratic and cubic Chebyshev approximating polynomials for τ_f as a function of the normalized final distance ratio $\tilde{\pi}_x$, are determined in Eqs. (33) and (34), respectively.

$$P_2(\tilde{\pi}_x) = 1.09191 + 0.170312\tilde{\pi}_x + 0.0780855\tilde{\pi}_x^2 \tag{33}$$

$$\begin{aligned} P_3(\tilde{\pi}_x) =& 1.09025 + 0.161437\tilde{\pi}_x + 0.0817668\tilde{\pi}_x^2 \\ &+ 0.0123006\tilde{\pi}_x^3 \end{aligned} \tag{34}$$

3.2 Least Squares Approximation

Another strategy for function approximation that is worth considering is the least squares method. In this method, the sum of the squares of the residuals, given in Eq. (35) is minimized to yield the polynomial given in Eq. (36) with small average error over the interval of approximation.

$$S_r = \sum_{i=1}^{n} \left(y_i - \left(c_0 + c_1\tilde{x}_1 + ... + c_k\tilde{x}_i^k\right)\right)^2 \tag{35}$$

$$y = c_0 + c_1\tilde{x} + ... + c_k\tilde{x}^k \tag{36}$$

The quadratic and cubic least squares approximations of τ_f are given in Eqs. (37) and (38), respectively.

$$L_2(\tilde{\pi}_x) = 1.09068 + 0.168701\tilde{\pi}_x + 0.0799931\tilde{\pi}_x^2 \tag{37}$$

$$\begin{aligned} L_3(\tilde{\pi}_x) =& 1.09068 + 0.160818\tilde{\pi}_x + 0.0799931\tilde{\pi}_x^2 \\ &+ 0.0129855\tilde{\pi}_x^3 \end{aligned} \tag{38}$$

Chebyshev and least squares approximating polynomials are computed for π_x on interval [0.001, 0.17]. Figure 3 shows the numerical solution and approximated values of τ_f. It is apparent from Fig. 4 that both second and third order Chebyshev approximations provide better performance in terms of minimizing the maximum error compared with the respective polynomial order of the least squares approximations.

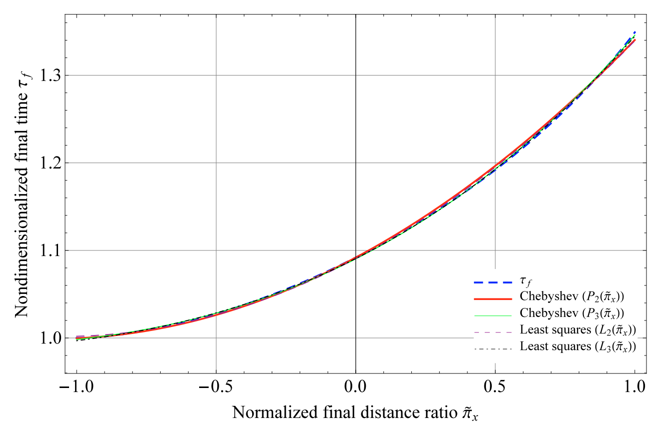

Fig. 3. Function approximation

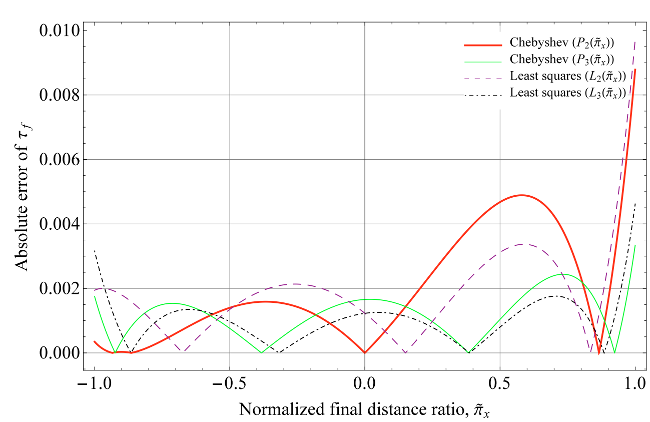

Fig. 4. Function approximation absolute error

Figure 5 shows the lower and upper bounds of the initial search interval for the Brent's method along with the computed τ_f. A search interval $[0.99P_3(\tilde{\pi}_x), 1.01P_3(\tilde{\pi}_x)]$ is reasonable because it is not too wide or too narrow.

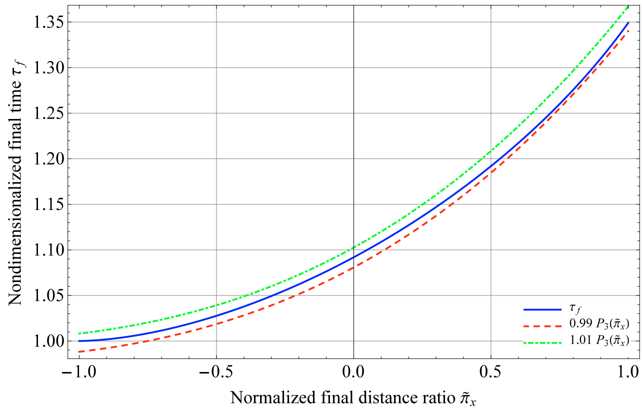

Fig. 5. Lower and upper bounds of the initial search interval

Figure 6 presents the number of function evaluations the Brent's method requires to converge. The iterations with interval $[\tau_{fl}, \tau_{fu}]$ converge if abs$((\tau_{fu} - \tau_{fl})/2) \leq$ tol, where tol $= 2.0\epsilon \max(\text{abs}(\tau_{fu}), 1.0)$, and ϵ is the machine epsilon (Moler, 2004). For the same search interval and convergence criteria, bisection method requires 48 function evaluations. Figure 6 shows the maximum number of function evaluations is 14, indicate the remarkable performance of the Brent's method with function approximation based search interval.

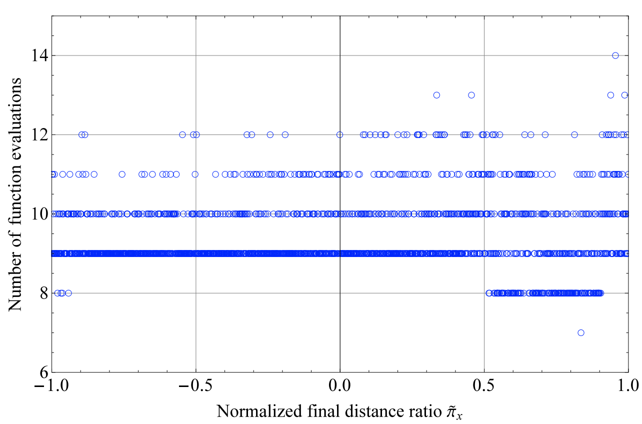

Fig. 6. Number of function evaluations

4. TOTAL VEHICLE FORCE AND MAXIMUM JERK

The total vehicle force can be represented in dimensionless form π_F, as shown in Eq. (40), by substituting Eq. (39) into Eq. (12) and using the definitions listed in Table 1. Once π_F is evaluated, F_t required to perform the obstacle avoidance maneuver can be calculated from Eq. (39).

$$F_t = \frac{mv_{x0}^2}{y_f}\pi_F \tag{39}$$

$$\pi_F = \frac{R^{3/2}\pi_x}{2N_1N_2P + \sqrt{R}\,(N_1^2N_2 + Q)} \tag{40}$$

The total vehicle forces for pure braking and pure steering are as given in Eqs. (41) and (42), respectively.

$$F_{tb} = \frac{mv_{x0}^2}{2x_f} \tag{41}$$

$$F_{ts} = \frac{4mv_{x0}^2 y_f}{x_f^2} \tag{42}$$

These forces can be expressed in dimensionless form using the definition in Eq. (39). The dimensionless total vehicle forces for pure steering and pure braking are denoted by π_{Fs} and π_{Fb}, respectively.

$$\pi_{Fs} = 4\pi_x^2 \tag{43}$$

$$\pi_{Fb} = \frac{1}{2}\pi_x \tag{44}$$

Figure 7 compares the dimensionless total vehicle force for steering with braking, pure steering, and pure braking cases. Switching point A at $\pi_x = 1/8$ is determined by algebraically solving $\pi_{Fs} = \pi_{Fb}$, whereas at switching point B, $\pi_x = 0.1716314$ is obtained by numerically solving $\pi_F = \pi_{Fb}$. These switching points provide essential insights into the selection of the best maneuver. If $\pi_x < 1/8$, pure steering is better than pure braking because a smaller total vehicle force is required. If $\pi_x > 1/8$, pure braking is better than pure steering. Similarly, if $\pi_x < 0.1716314$, steering with braking requires a smaller total vehicle force compared with pure braking, and pure braking becomes the optimal maneuver when $\pi_x > 0.1716314$. Interestingly, Fig. 7 demonstrates the lower and upper bounds on π_x for steering with braking to be the most effective maneuver. Another significant application of Fig. 7 is that one can continuously monitor the required F_t and compare it with $F_{\max}$ available.

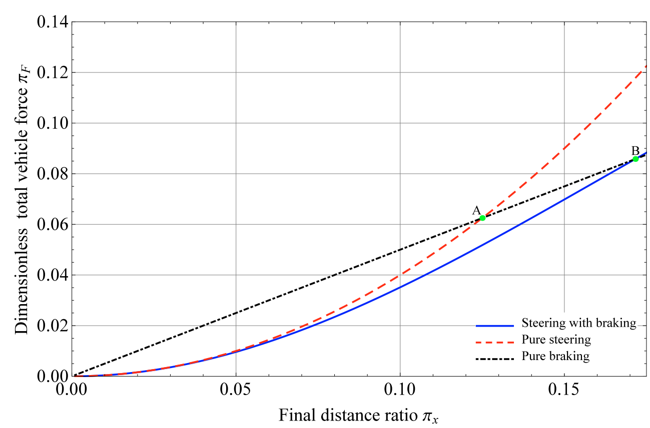

Fig. 7. Dimensionless total vehicle force for steering with braking, pure steering and pure braking cases

Figure 8 illustrates the variation of F_t with respect to v_{x0} at $y_f = 3.5$ m and $m = 1707$ kg for different values of x_f. For a given v_{x0}, the F_t required to execute the lane change maneuver decreases with the increase in x_f.

Jerk is defined as the time derivative of acceleration. A trapezoidal acceleration profile that accommodates the maximum lateral acceleration and maximum lateral jerk constraints was proposed for the automated lane change maneuver (Chee and Tomizuka, 1994). In their study, lateral jerk of 1 m/s^3 was considered for human comfort. Isermann et al. (2008) used a sigmoide function to represent a collision avoidance vehicle position trajectory that

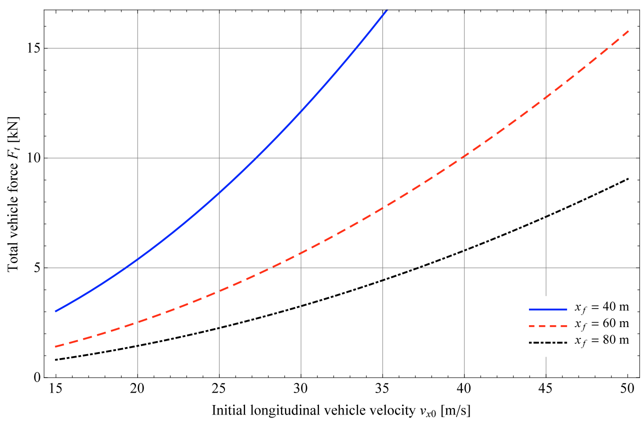

Fig. 8. Total vehicle force for different final longitudinal distances

captures the limits on the lateral acceleration and lateral jerk. Lateral jerk of 30 m/s^3 was considered for evasive maneuver. Therefore, jerk is an important aspect for the collision avoidance study.

In the present study, we provide a mathematical relation between the jerks along the trajectory with respect to v_{x0}, x_f, and y_f. The longitudinal jerk along the trajectory is obtained by differentiating Eq. (9) with respect to t.

$$j_x = \frac{F_t}{m} \frac{\nu_v \left(\nu_y \left(t_f - t\right) + \nu_v\right)}{\left(\left(t - t_f\right)^2 + \left(\nu_y \left(t_f - t\right) + \nu_v\right)^2\right)^{3/2}} \tag{45}$$

By differentiating Eq. (45) with respect to t and then equating the differentiated equation to zero, a quadratic equation in t is obtained. By solving this equation for t, we have

$$\left.\begin{matrix} t_{x1} \\ t_{x2} \end{matrix}\right\} = \frac{4\nu_y t_f \left(\nu_y^2 + 1\right) + \nu_v \left(4\nu_y^2 + 3 \pm \sqrt{8\nu_y^2 + 9}\right)}{4\nu_y \left(\nu_y^2 + 1\right)} \tag{46}$$

Therefore, two extremum longitudinal jerks occur at t_{x1} and t_{x2}.

$$\left.\begin{matrix} j_{x1} \\ j_{x2} \end{matrix}\right\} = \frac{4F_t}{3m}\sqrt{\frac{2}{3}} \frac{\nu_y^2 \sqrt{\nu_y^4 + \nu_y^2} \left(1 \mp \sqrt{8\nu_y^2 + 9}\right)}{\nu_v \left(4\nu_y^2 + 3 \pm \sqrt{8\nu_y^2 + 9}\right)^{3/2}} \tag{47}$$

Differentiating Eq. (10) with respect to t yields the lateral jerk during the maneuver

$$j_y = \frac{F_t}{m} \frac{\nu_v \left(t - t_f\right)}{\left(\left(t - t_f\right)^2 + \left(\nu_y \left(t_f - t\right) + \nu_v\right)^2\right)^{3/2}} \tag{48}$$

Equation (48) is differentiated with respect to t and the result is equated to zero. This produces a quadratic equation in t, which when solved gives

$$\left.\begin{matrix} t_{y1} \\ t_{y2} \end{matrix}\right\} = \frac{4t_f \left(\nu_y^2 + 1\right) \pm \nu_v \left(\nu_y + \sqrt{9\nu_y^2 + 8}\right)}{4\left(\nu_y^2 + 1\right)} \tag{49}$$

The lateral jerks at t_{y1} and t_{y2} are expressed as

$$\left.\begin{matrix} j_{y1} \\ j_{y2} \end{matrix}\right\} = \frac{4F_t}{3m}\sqrt{\frac{2}{3}} \frac{\sqrt{\nu_y^2 + 1} \left(\nu_y \pm \sqrt{9\nu_y^2 + 8}\right)}{\nu_v \left(4 + \nu_y \left(3\nu_y \mp \sqrt{9\nu_y^2 + 8}\right)\right)^{3/2}} \tag{50}$$

Because the total acceleration is constant, the total jerk j_t, is proportional to the angular velocity $\dot{\varphi}$.

$$j_t = \frac{F_t}{m}\dot{\varphi}(t) \tag{51}$$

In order to find the maximum total jerk, the derivative of Eq. (51) with respect to t is equated to zero, and the resulting equation is solved with respect to t.

$$t_1 = t_f + \frac{\nu_y \nu_v}{\nu_y^2 + 1} \tag{52}$$

At t_1, the total jerk is

$$j_{t1} = \frac{F_t}{m}\frac{\nu_y^2 + 1}{\nu_v} \tag{53}$$

In order to verify whether these maximum jerks occur within interval $[t_0, t_f]$, Eqs. (46), (49) and (52) should first be translated to the respective dimensionless time.

$$\left.\begin{matrix} \tau_{x1} \\ \tau_{x2} \end{matrix}\right\} = \frac{4N_1\tau_f R + N_2\left(4N_1^2 + 3 \pm \sqrt{8N_1^2 + 9}\right)}{4N_1 R} \tag{54}$$

$$\left.\begin{matrix} \tau_{y1} \\ \tau_{y2} \end{matrix}\right\} = \frac{N_1 N_2 + 4\tau_f R \pm N_2\sqrt{9N_1^2 + 8}}{4R} \tag{55}$$

$$\tau_{t1} = \tau_f + \frac{N_1 N_2}{R} \tag{56}$$

Then, by plotting Eqs. (54) to (56) along with τ_f in the same figure, the maximum jerks that occur outside interval $[t_0, t_f]$ can be detected and omitted. Figure 9 shows that only $\tau_{y1} > \tau_f$ indicate that j_{y1} does not occur along the trajectory.

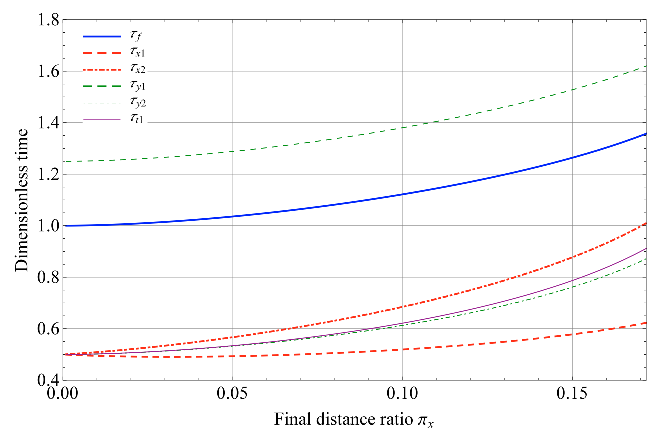

Fig. 9. Dimensionless time for maximum jerks and dimensionless final time against final distance ratio

The maximum longitudinal jerks can be expressed in dimensionless form

$$\left.\begin{matrix} J_{x1} \\ J_{x2} \end{matrix}\right\} = \frac{4}{3}\sqrt{\frac{2}{3}} \frac{N_1^2 \pi_F \pi_x \sqrt{RN_1^2}\left(1 \mp \sqrt{8N_1^2 + 9}\right)}{N_2\left(4N_1^2 + 3 \pm \sqrt{8N_1^2 + 9}\right)^{3/2}} \tag{57}$$

Similarly, the dimensionless maximum lateral jerk is

$$J_{y2} = \frac{4}{3}\sqrt{\frac{2}{3}} \frac{\pi_F \pi_x \sqrt{R}\left(N_1 - \sqrt{9N_1^2 + 8}\right)}{N_2\left(4 + N_1\left(3N_1 + \sqrt{8N_1^2 + 9}\right)\right)^{3/2}} \tag{58}$$

and the dimensionless maximum total jerk is

$$J_{t1} = \frac{R\pi_F\pi_x}{N_2} \tag{59}$$

Figure 10 presents the dimensionless maximum longitudinal, lateral, and total jerks as functions of π_x. Note that these jerks can be easily computed after the numerical solution of τ_f is obtained. In general, the absolute values of the dimensionless jerks increases as π_x increases. For a given y_f, starting an automated lane change maneuver with shorter x_f will produce higher jerks. Figures 7 and 10 are important tools for verifying whether the constraints on the total vehicle force and jerks are violated for a given π_x.

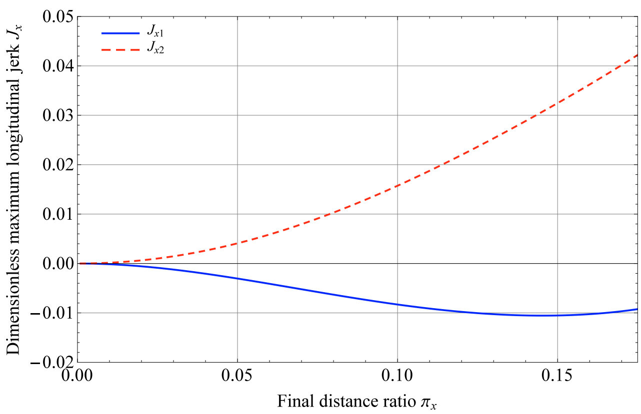

(a) Dimensionless maximum longitudinal jerks

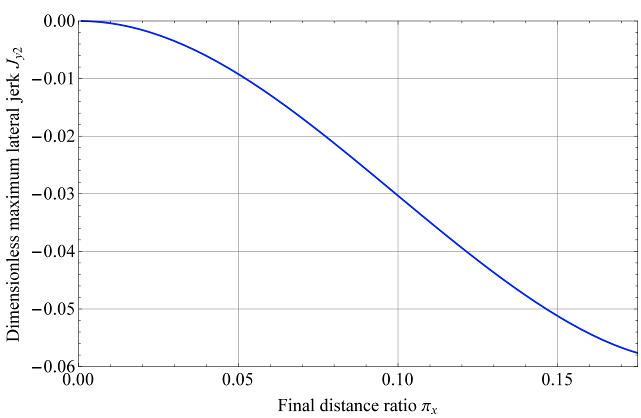

(b) Dimensionless maximum lateral jerk

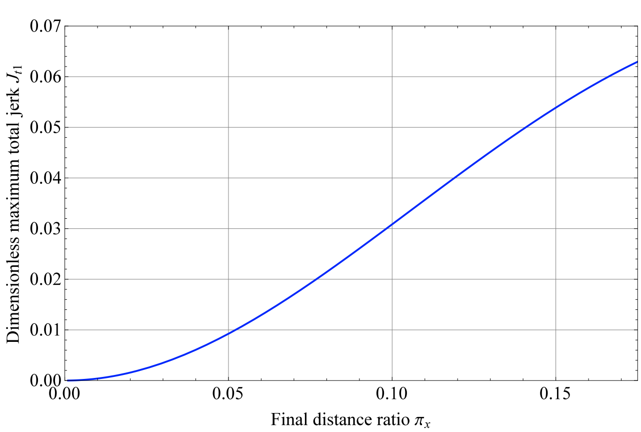

(c) Dimensionless maximum total jerk

Fig. 10. Dimensionless jerks for given final distance ratio

A numerical example of the jerks along the trajectory for $v_{x0} = 25$ m/s, $x_f = 40$ m, and $y_f = 3$ m is shown in Fig. 11. It can be seen that the maximum jerks occur approximately at the trajectory midway.

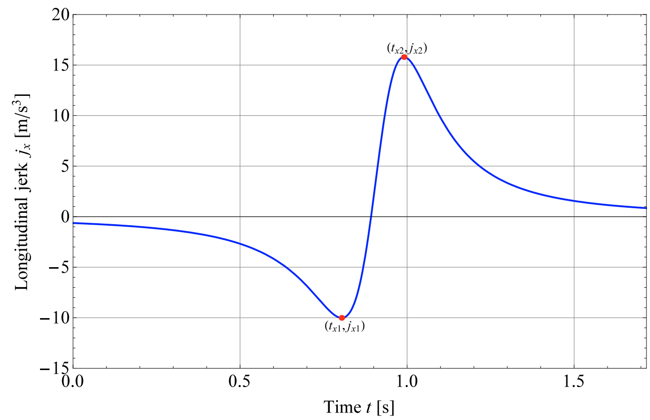

(a) Longitudinal jerk

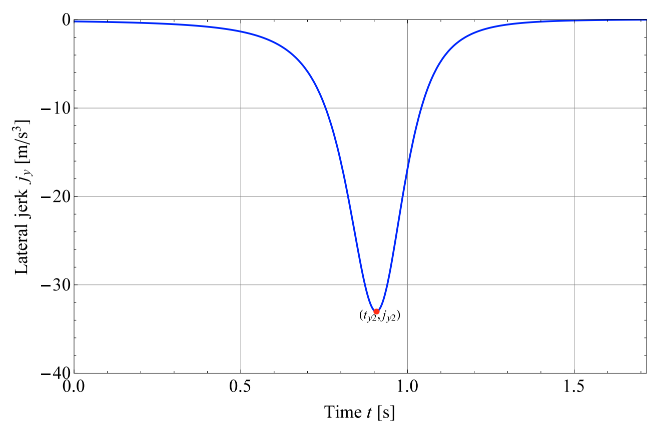

(b) Lateral jerk

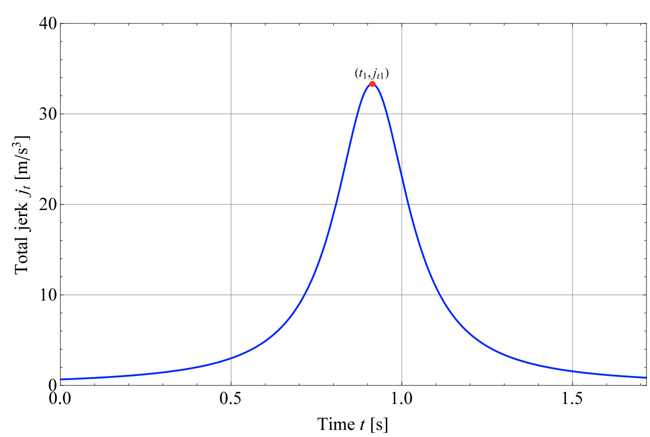

(c) Total jerk

Fig. 11. Jerk profiles

5. CONCLUSIONS

Optimal control for automatic single lane change maneuver by minimizing the total force of the vehicle is developed. The effectiveness of the nondimesionalization in reducing the complexity of the obstacle avoidance problem is clearly demonstrated. Fast and robust Brent's method with function approximation for setting the search interval was used in order to obtain a precise solution of the one equation in one unknown problem. The relations between the total vehicle force and jerk, and vehicle states are established in a dimensionless domain. Further studies that consider a more general problem setting with nonzero initial lateral velocity for the realization of feedback controller will be undertaken.

ACKNOWLEDGEMENTS

The first author received an Academic Training Scheme scholarship from the Ministry of Higher Education Malaysia (MOHE) and Universiti Teknikal Malaysia Melaka (UTeM).

REFERENCES

Alvarez, L., Yi, J., Horowitz, R., and Olmos, L. (2004). Dynamic friction model-based tire-road friction estimation and emergency braking control. *Journal of Dynamic Systems, Measurement, and Control, Transactions of the ASME*, 127(1), 22–32.

Brent, R.P. (1971). An algorithm with guaranteed convergence for finding a zero of a function. *The Computer Journal*, 14(4), 422–425.

Bryson, A. and Ho, Y.C. (1975). *Applied Optimal Control: Optimization, Estimation and Control*. Taylor & Francis, New York.

Chee, W. and Tomizuka, M. (1994). Lane change maneuver for AHS applications. In *International Symposium on Advanced Vehicle Control. AVEC 1994*, 420–425.

Fujioka, T., Shibata, Y., Tsukasaki, Y., and Sawada, S. (2008). Vehicle motion control for minimizing collision risk by use of optimal control theory. In *2008 JSAE Annual Congress (Spring)*, 21–26. (in Japanese).

Hattori, Y. and Ohmuro, A. (2010). Optimum vehicle trajectory control for obstacle avoidance - feedback controllers for various objective functions. In *International Symposium on Advanced Vehicle Control. AVEC 2010*, 267–272.

Hattori, Y., Ono, E., and Hosoe, S. (2008). An optimum vehicle trajectory control for obstacle avoidance with the shortest longitudinal traveling distance. In *IEEE International Conference on Mechatronics and Automation, 2008. ICMA 2008*, 13–20.

Horiuchi, S., Hirao, R., Okada, K., and Nohtomi, S. (2006). Optimal steering and braking control in emergency obstacle avoidance. *Transactions of the Japan Society of Mechanical Engineers Series C*, 72(722), 3250–3255. (in Japanese).

Isermann, R., Schorn, M., and Stählin, U. (2008). Anticollision system PRORETA with automatic braking and steering. *Vehicle System Dynamics*, 46(sup1), 683–694.

Moler, C. (2004). *Numerical Computing with Matlab, Revised Reprint*. Society for Industrial and Applied Mathematics.

Muller, S., Uchanski, M., and Hedrick, K. (2003). Estimation of the maximum tire-road friction coefficient. *Journal of Dynamic Systems, Measurement and Control, Transactions of the ASME*, 125(4), 607–617.

Nishihara, O. and Higashino, S. (2013). Exact optimization of four-wheel steering and four-wheel independent driving/braking force distribution with minimax criterion of tire workload. *Transactions of the Japan Society of Mechanical Engineers Series C*, 79(799), 629–644. (in Japanese).

Nishihara, O. and Kurishige, M. (2011). Estimation of road friction coefficient based on the brush model. *Journal of Dynamic Systems, Measurement and Control, Transactions of the ASME*, 133(4), 041006–1–041006–9.

Ohmuro, A. and Hattori, Y. (2010). Optimum vehicle trajectory control for obstacle avoidance - a minimax problem of resultant vehicle force). *Transactions of the Japan Society of Mechanical Engineers Series C*, 76(772), 3587–3594. (in Japanese).

Ono, E., Hattori, Y., Muragishi, Y., and Koibuchi, K. (2006). Vehicle dynamics integrated control for four-wheel-distributed steering and four-wheel-distributed traction/braking systems. *Vehicle System Dynamics*, 44(2), 139–151.

Press, W.H., Teukolsky, S.A., Vetterling, W.T., and Flannery, B.P. (1992). *Numerical Recipes in C (2nd Ed.): The Art of Scientific Computing*. Cambridge University Press, New York.

Shiller, Z. and Sundar, S. (1998). Emergency lane-change maneuvers of autonomous vehicles. *Journal of Dynamic Systems, Measurement and Control, Transactions of the ASME*, 120(1), 37–44.

Singh, A.S.P. and Nishihara, O. (2016). Nondimensionalized indices for collision avoidance based on optimal control theory. In *FISITA 2016 World Automotive Congress*. (Accepted).

Wang, J., Alexander, L., and Rajamani, R. (2004). Friction estimation on highway vehicles using longitudinal measurements. *Journal of Dynamic Systems, Measurement and Control, Transactions of the ASME*, 126(2), 265–275.